KAONIC ATOMS — RESULTS OF THE SIDDHARTA EXPERIMENT*

T. Ishiwatari, C. Berucci, M. Cargnelli, J. Marton, H. Shi, E. Widmann
J. Zmeskal

Stefan-Meyer-Institut für Subatomare Physik, Austria

M. Bazzi, C. Curceanu, A. d'Uffizi, C. Guaraldo, M. Iliescu, P. Levi Sandri
E. Sbardella, A. Scordo, H. Tatsuno

INFN, Laboratori Nazionali di Frascati, Italy

G. Beer

Department of Physics and Astronomy, University of Victoria, Canada

C. Fiorini, R. Quaglia

Politecnico di Milano, Dipartimento di Elettronica, Informazione e Bioingegneria and
INFN Sezione di Milano, Milano, Italy

A.M. Bragadireanu, D. Pietreanu, D.L. Sirghi, F. Sirghi

INFN, Laboratori Nazionali di Frascati, Italy
and IFIN-HH, Inst. Nat. pentru Fizica si Inginerie Nucleara Horia Hulubei, Romania

F. Ghio

INFN Sezione di Roma I and Instituto Superiore di Sanita, Italy

R.S. Hayano

University of Tokyo, Japan

M. Iwasaki, S. Okada

RIKEN, Institute of Physical and Chemical Research, Japan

P. Kienle

Excellence Cluster Universe, Technische Universität München, Germany

T. Ponta, A. Tudorache, V. Tudorache

IFIN-HH, Inst. Nat. pentru Fizica si Inginerie Nucleara Horia Hulubei, Romania

A. Romero Vidal

Universidade de Santiago de Compostela, Spain

O. Vazquez Doce

INFN, Laboratori Nazionali di Frascati, Italy
and Excellence Cluster Universe, Technische Universität München, Germany

(Received January 7, 2014)

* Presented at the II International Symposium on Mesic Nuclei, Kraków, Poland, September 22–25, 2013.

Studies of the low-energy $\bar{K}N$ interaction have been performed based on X-ray spectroscopy of light kaonic atoms by the SIDDHARTA experiment, where the K-series lines of kaonic hydrogen and deuterium, and the L-series lines of kaonic ^{3}He and ^{4}He were measured, as well as kaonic atom X-ray transitions produced in Kapton. This article deals with the short summary of the results of these measurements in the SIDDHARTA experiment.

DOI:10.5506/APhysPolB.45.787
PACS numbers: 13.75.Jz, 29.30.Kv, 32.30.Rj, 36.10.Gv

1. Introduction

X-ray spectroscopy of kaonic atoms plays an important role for understanding the low-energy $\bar{K}N$ interaction at threshold. The SIDDHARTA experiment, which was performed at LNF (Italy), measured X-ray lines from four light kaonic atoms at around 6-keV energy using silicon drift detectors (SDDs) as X-ray detectors and gaseous targets. The most precise values of the shift and width of the kaonic hydrogen 1s state were determined [1, 2], as well as the upper limit of the kaonic deuterium K-series lines [3]. Also, the shifts and widths of kaonic helium isotopes (3 and 4) were determined [4–7]. In addition to the measurements with gaseous targets, kaonic atom X-rays produced in the target wall made of Kapton were measured [8]. In this article, the results reported above are briefly summarized.

2. Experiment

Kaonic atom X-rays using gaseous targets were measured by the SIDDHARTA experiment at DAΦNE in LNF (Italy). DAΦNE is an electron–positron collider, which is optimized to produce at-rest ϕ-mesons at the interaction point. Because of the decay modes of ϕ-mesons, low-energy and monochromatic charged kaon pairs (K^+K^-) were produced with a branching ratio of about 50%. The property of these negatively charged kaons (K^-) is suited for production of kaonic atoms, and thereby gaseous targets can be used [9].

Figure 1 shows the schematic view of the SIDDHARTA experimental setup. At the DAΦNE interaction point, electrons and positrons collided, and almost at-rest ϕ mesons were created. K^+K^- pairs produced by ϕ decay were emitted from the interaction point. The K^+K^- pairs were detected by a kaon detector consisting of two plastic scintillators placed above and below the beam pipe. The timing signals of the K^+K^- pairs were recorded using clock signals with a frequency of 120 MHz generated by DAΦNE. Because of a finite crossing angle of the electron and position beams, the momentum of the emitted kaons had an angular dependence. This angular dependence was

compensated using a stepped degrader made of Mylar foils with thicknesses ranging from 100 to 800 μm which were optimized to increase kaon stops in the target gas.

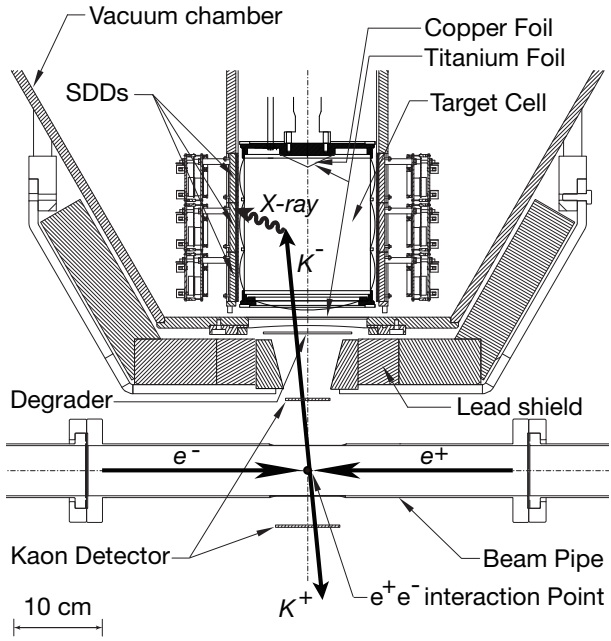


Fig. 1. Schematic view of the experimental setup.

The charged kaons entered the target cell after passing through the scintillator and degrader. The cylindrical target cell was made of Kapton polyimide ($C_{22}H_{10}N_2O_5$) foils with a thickness of 75 μm and a density of 1.42 g/cm^3. The size of the cell had 15.5 cm high with a diameter of 13.7 cm. The bottom of the target cell, through which the charged kaons entered, was also made of Kapton. On the top of the target cell, thin Ti and Cu foils were installed to produce fluorescence X-rays induced by the beam background.

The X-rays were measured by silicon drift detectors (SDDs) [10], which surrounded the target. Each SDD has an effective area of 1 cm^2 with a 450-μm thickness. There were 144 SDDs in total. The SDDs were cooled to a temperature of 170 K to obtain an excellent energy resolution of about 150 eV for 6 keV X-rays, which is close to the resolution in noise-free conditions.

The data on the kaonic atom X-rays were accumulated in 2009. In the experiment, we used four target gases: hydrogen (1.30 g/l), deuterium (2.50 g/l), helium-3 (0.96 g/l) and helium-4 (1.65 g/l and 2.15 g/l). They were cooled to 23 K. The charged kaons stopped mainly in the target gas and partially in the Kapton windows.

3. Data analysis

The data taken with the SDDs and the kaon detector were analyzed to extract kaonic atom X-ray spectra. The calibration data were taken with the Ti and Cu foils excited by an X-ray tube and the beam background. Using high statistics of the fluorescence Ti and Cu X-rays, the energy scale was calibrated for each SDD (see Fig. 2 (a)). In addition to the energy calibration, the time dependent instability was also corrected. The energy calibration and the instability correction were performed every few hours. Among the 144 SDDs, 94 were selected for further analysis based on energy resolution, stability, and peak shapes.

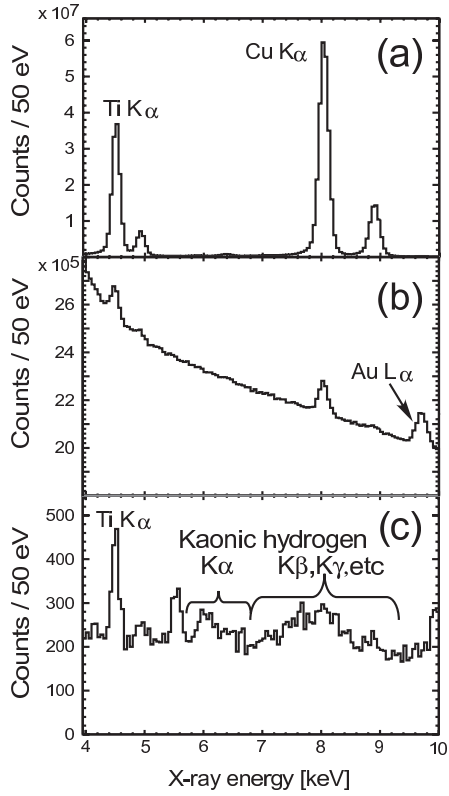


Fig. 2. Energy spectra measured in SIDDHARTA. (a) Energy spectrum taken with the beam background and the X-ray tube irradiation. (b) Energy spectrum with timing uncorrelated to K^+K^- pairs. (c) Energy spectrum with timing selections.

Figure 2 (b) shows the energy spectrum obtained with 94 SDDs with timing uncorrelated to the K^+K^- pairs. Together with the large beam background, there are fluorescence X-ray peaks at 4.5, 8.0, and 9.6 keV,

which were identified as the Ti $K\alpha$, Cu $K\alpha$ and Au $L\alpha$ lines. The Ti and Cu lines were produced in the foils installed on the top of the target cell, while the Au line was produced in the material of the printed-circuit boards of the SDDs.

The accuracy of the energy scale determined using the calibration data was examined using these three peak positions. The fit of the X-ray peaks showed that the gain was slightly shifted by about 6 eV. This gain shift was expected because the hit rates of the SDDs were much higher in the calibration data. The gain shift was corrected with an accuracy of ± 4 eV.

With timing cuts on the SDDs and event selection on the K^+K^- pairs in the kaon detector, a clean energy spectrum of the kaonic atom X-rays was extracted. Figure 2 (c) shows the energy spectrum using the hydrogen gas target. The bumps from 6 keV to 9 keV were identified as X-ray signals from kaonic hydrogen. The sharp peaks were attributed to X-ray transitions in the kaonic atoms produced in Kapton.

4. Kaonic hydrogen and deuterium

The results of kaonic hydrogen experiments performed by the KpX [11] and DEAR [12] collaborations showed the negative sign of the strong-interaction shift on the kaonic hydrogen 1s state. The DEAR experiment obtained the shift with the most precise value. However, the result obtained by DEAR is not in a good agreement with theoretical calculations using scattering data, branching ratios, *etc.* In particular, the behavior below the K^-p threshold is very sensitive to constraints with/without the DEAR result [13]. Therefore, it is very important to determine the shift and width of the kaonic hydrogen 1s state with a better accuracy.

Figure 3 shows the energy spectrum taken with hydrogen gas in the SIDDHARTA experiment, where the continuous background and the X-ray transition lines from Kapton were subtracted. The peak position of the $K\alpha$ line is clearly seen at lower than the X-ray energy calculated using the electro-magnetic interaction only (EM value), meaning that the strong-interaction shift can be determined to be negative.

To determine the shift and width of the kaonic hydrogen 1s state, the energy spectrum of kaonic hydrogen was fitted using the Voigt function, which is a convolution of Gaussian and Lorentzian. The Gaussian function represents the detector response function, whose parameters were determined from the calibration data. Because the strong-interaction shifts and widths of np ($n > 1$) states are expected to be very small, a common shift and a common width were used in the fit. The determination of the shift and width of the kaonic hydrogen 1s state was performed using the $K\alpha$ and $K\beta$ lines, whereas contributions from the K-high transitions (*i.e.*, $K\gamma$, $K\delta$, *etc.*) were taken as part of background.

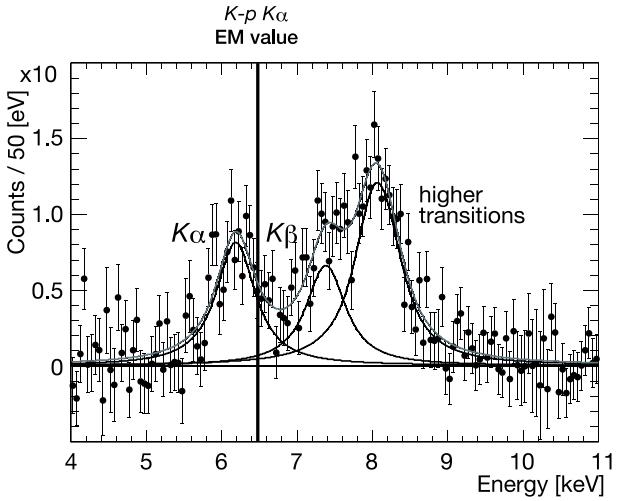


Fig. 3. Energy spectra of kaonic hydrogen.

With the fit of the energy spectrum, the strong-interaction shift and width of the kaonic hydrogen $1s$ state were determined to be

$$\epsilon_{1s} = -283 \pm 36 \text{ (stat.)} \pm 6 \text{ (syst.) eV}, \quad (1)$$

$$\Gamma_{1s} = 541 \pm 89 \text{ (stat.)} \pm 22 \text{ (syst.) eV}. \quad (2)$$

Measurements of the shift and width of the kaonic deuterium $1s$ state are very important to determine the isospin dependent scattering lengths a_0 and a_1. The first measurement of kaonic deuterium was performed in the SIDDHARTA experiment. However, due to a limited signal-to-background ratio, no clear signals from kaonic deuterium were observed. Compared to Monte Carlo simulations, the upper limits of the yield of the kaonic deuterium $K\alpha$ line was evaluated as

$$Y(K_\alpha) < 0.0039 \text{ (C.L. 90\%)}, \quad (3)$$

where theoretically expected shift and width values were used in the fit. The determined limit is consistent with cascade calculations. These results are important for the evaluation of the new experiments proposed at LNF [14] and J-PARC [15].

5. Kaonic ^{3}He and ^{4}He

The X-ray measurements of kaonic ^{4}He atoms performed in the 70s and 80s introduced a serious problem; *i.e.*, inconsistency between theory and experiment both in the shift and width of the kaonic ^{4}He $2p$ state [16]. The

shift measured in the 70s and 80s was 43 ± 8 eV on average, whereas theoretical calculations gave a shift below 1 eV based on the kaonic atom data with the atomic numbers $Z \geq 3$ [16, 17]. The widths of $\Gamma_{2p} = 1$–2 eV was theoretically estimated both for kaonic ^{3}He and ^{4}He. Experimentally, however, the width of kaonic ^{4}He was not well determined, leaving the situation unclear with the average of 55 ± 34 eV [16].

The discrepancy of the shift and width between theory and experiment is known as the "kaonic helium puzzle". Possible shifts up to 10 eV and widths up to 40 eV either in kaonic ^{3}He or ^{4}He were calculated related to the kaonic nuclear systems [19, 20]. Therefore, it is very important to perform a precision measurement of the shift and width of the kaonic ^{4}He $2p$ state, and for the first time of kaonic ^{3}He.

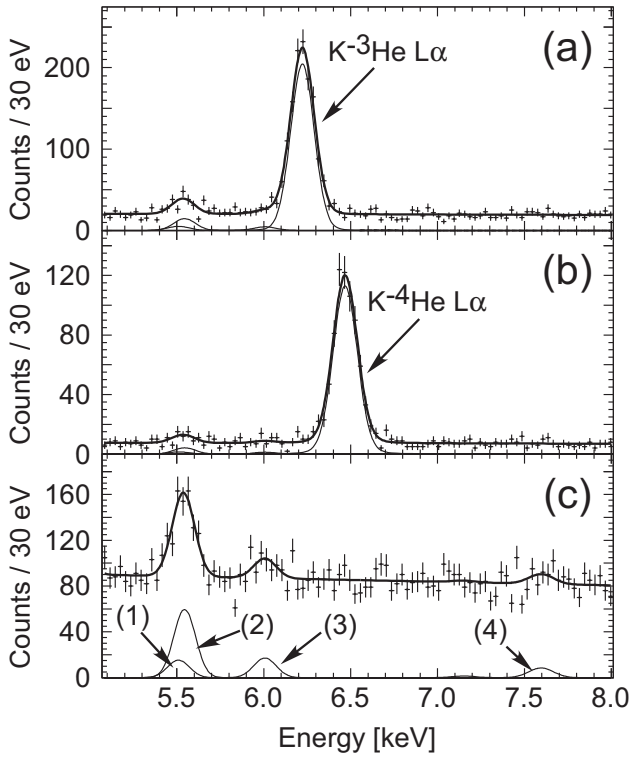


Fig. 4. X-ray energy spectra of (a) kaonic ^{3}He, (b) kaonic ^{4}He, and (c) kaonic deuterium. The thin lines show the peak fit functions after the background subtraction. The positions of the kaonic ^{3}He and ^{4}He $3d \to 2p$ transitions are shown. In Fig. (c), (1): kaonic carbon $6 \to 5$ transition, (2): kaonic carbon $8 \to 6$ transition, (3): kaonic oxygen $7 \to 6$ transition, and (4): kaonic nitrogen $6 \to 5$ transition.

The energy spectra of the kaonic ^{3}He and ^{4}He X-rays are shown in Figs. 4 (a) and (b), where the thin lines show the peak fit functions after the background subtraction. The peaks at 6.2 keV and 6.4 keV are the kaonic ^{3}He and ^{4}He $3d \to 2p$ transitions, respectively. Figure 4 (c) shows the X-ray energy spectrum using the deuterium target, where the signals of the kaonic deuterium X-rays are not visible.

In addition to kaonic helium, several small peaks were observed in all the spectra, which originated from the kaonic atom X-rays produced in the target window material made of Kapton polyimide ($C_{22}H_{10}N_2O_5$). The kaonic ^{3}He X-ray peak partially overlapped with the K^-O transition. The contamination of this transition was evaluated using the kaonic deuterium data.

The energy spectra were fitted using a Voigt function: $V = V(\sigma, \Gamma)$, where Γ represents the strong-interaction $2p$ width. Due to the strong parameter correlation between the values of σ and Γ in the fit, the values of σ were fixed using the values obtained from the calibration data. The main contribution to the systematic errors for the widths is related to the uncertainty in the values of the detector response. The determined shift and width of the kaonic helium $2p$ states are summarized in Table I, together with the results of the previous experiments. Our results are inconsistent with the previous experiments, whereas they are consistent with theoretical predictions. Therefore, the "kaonic helium" puzzle was resolved both for the shift and width.

TABLE I

Energy shifts (ΔE_{2p}) and widths (Γ_{2p}) of the kaonic helium ^{3}He and ^{4}He $2p$ states.

Target	ΔE_{2p} [eV]	Γ_{2p} [eV]	Ref.
^{4}He	-41 ± 33	—	Wiegand *et al.* [22]
^{4}He	-35 ± 12	30 ± 30	Batty *et al.* [23]
^{4}He	-50 ± 12	100 ± 40	Baird *et al.* [24]
^{4}He	-43 ± 8	55 ± 34	Average of above [16, 24]
^{4}He	$+2 \pm 2$ (stat.) ± 2 (syst.)	—	Okada *et al.* [25]
^{4}He	0 ± 6 (stat.) ± 2 (syst.)	—	SIDDHARTA [5]
^{4}He	$+5 \pm 3$ (stat.) ± 4 (syst.)	14 ± 8 (stat.) ± 5 (syst.)	SIDDHARTA [4, 6]
^{3}He	-2 ± 2 (stat.) ± 4 (syst.)	6 ± 6 (stat.) ± 7 (syst.)	SIDDHARTA [4, 6]

6. Kaonic atoms produced in Kapton

Together with the kaonic atom X-rays produced in the gaseous targets, kaonic atom X-rays produced in the target window made of Kapton were observed in the same time. Because Kapton contains C, N, O atoms, X-rays from kaonic carbon, kaonic nitrogen and kaonic oxygen atoms were expected to be measured.

Although these X-ray transitions do not significantly influence on the strong interaction, X-ray yields of these kaonic atoms are of interest, related to kaon capture ratios and cascade processes in compound materials. However, there were no X-ray yield data in such complex compounds. In addition, it is reported that the X-ray yields are strongly related to atomic number Z, as well as the composition materials such as hydrogen [26, 27].

Figure 5 shows the energy spectrum taken with the deuterium gas. Compared to Monte Carlo simulations, the absolute X-ray yields of kaonic atoms produced in Kapton were determined for the first time [8]. Table II shows the absolute X-ray yield Y of the kaonic atoms produced in Kapton. Special care was taken of defining X-ray yields in Kapton. When a kaon stops in Kapton ($C_{22}H_{10}N_2O_5$), it results in X-rays from one of kaonic carbon, nitrogen, oxygen or hydrogen. However, there is a lack of knowledge on which atom first captures the kaon. To account for this, we define the X-ray yields as the number of X-rays per stopped K^- in $C_{22}H_{10}N_2O_5$.

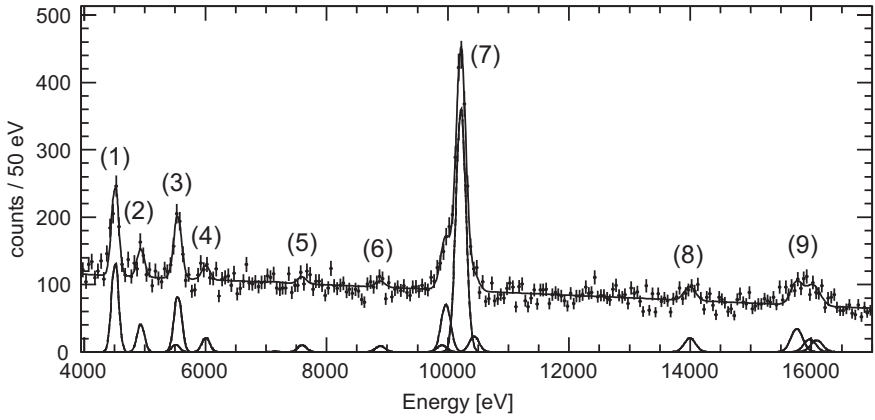


Fig. 5. Energy spectrum of the kaonic atom X-rays produced in Kapton, where the target cell was filled with deuterium. (1) Ti $K\alpha$, (2) Ti $K\beta$, (3) kaonic carbon (K^-C) $8 \to 6$ and $6 \to 5$, (4) kaonic oxygen (K^-O) $7 \to 6$, (5) kaonic nitrogen (K^-N) $6 \to 5$, (6)K^-N $7 \to 5$, (7)K^-O $8 \to 6$ and $6 \to 5$, K^-C $5 \to 4$, and kaonic aluminium (K^-Al) $8 \to 7$, (8)K^-N $5 \to 4$, and (9) K^-C $6 \to 4$, K^-O $7 \to 5$, and K^-Al $7 \to 6$ transitions.

TABLE II

X-ray yields Y of the kaonic atoms produced in Kapton. The X-ray yields Y were defined as the number of X-rays per stopped K^- in $C_{22}H_{10}N_2O_5$. The last column gives the X-ray yields Y normalized by the atomic percentages f_a.

Transition	Energy [keV]	Yield (Y) [%]	Y/f_a [%]
K^-C $5 \to 4$	10.2165	$9.7^{+0.7}_{-2.3}$	$17.3^{+1.2}_{-4.1}$
K^-C $6 \to 5$	5.5449	$2.2^{+0.6}_{-0.7}$	$4.0^{+1.1}_{-1.2}$
K^-C $6 \to 4$	15.7594	1.3 ± 0.3	2.4 ± 0.5
K^-C $7 \to 5$	8.8858	0.2 ± 0.2	0.4 ± 0.3
K^-C $8 \to 6$	5.5096	0.3 ± 0.6	0.5 ± 1.0
K^-N $5 \to 4$	13.9959	0.7 ± 0.2	$14.0^{+3.9}_{-4.8}$
K^-N $6 \to 5$	7.5954	0.2 ± 0.2	$4.7^{+3.2}_{-3.1}$
K^-O $6 \to 5$	9.9687	$1.8^{+0.4}_{-0.5}$	$14.2^{+3.0}_{-3.7}$
K^-O $7 \to 6$	6.0068	0.5 ± 0.2	4.2 ± 1.6
K^-O $7 \to 5$	15.9733	0.8 ± 0.3	6.0 ± 2.6
K^-O $8 \to 6$	9.9027	0.3 ± 0.3	$2.1^{+2.5}_{-2.6}$

The X-ray yields Y of kaonic nitrogen are smaller because of the small atomic percentage of nitrogen in Kapton ($f_a = 2/39$), as expected. The ratios of C:N:O in the X-ray yields are expected to be related to the atomic ratios of Kapton. The X-ray yields normalized by the atomic percentages f_a are shown in Table II. The normalized yields Y/f_a of kaonic carbon and kaonic nitrogen are almost the same within the errors both in the $5 \to 4$ and $6 \to 5$ transitions, while Y/f_a of the kaonic oxygen transitions are higher than those of kaonic carbon or kaonic nitrogen both in the $6 \to 5$ and $7 \to 5$ transitions.

The yield patterns and the yield ratios can be related to the capture processes in the Kapton compound and the cascade processes of the kaonic atoms. A detailed theoretical calculation is needed to understand the yield patterns determined in this experiment.

7. Summary

The SIDDHARTA experiment measured X-ray lines from kaonic hydrogen, deuterium, ^{3}He and ^{4}He. The most precise values of the shift and width of the kaonic hydrogen $1s$ state were determined. Compared to the Monte Carlo simulations, the upper limit of the X-ray yield of the kaonic deuterium $K\alpha$ line was evaluated. The shifts and widths of the kaonic ^{3}He and ^{4}He

were determined for the first time. In addition, the absolute yields of X-rays produced in Kapton were determined. Studies of the determination of the X-ray yields of kaonic hydrogen and helium isotopes are in progress. New experiments of kaonic deuterium are planned at LNF and J-PARC.

We thank C. Capoccia, B. Dulach, and D. Tagnani from LNF-INFN; and H. Schneider, L. Stohwasser, and D. Stückler from Stefan-Meyer-Institut, for their fundamental contribution in designing and building the SIDDHARTA setup. We thank also the DAΦNE staff for the excellent working conditions and permanent support. Part of this work was supported by the HadronPhysics I3 FP6 European Community program, Contract No. RII3-CT-2004-506078; HadronPhysics 2, Grant Agreement No. 227431, and the HadronPhysics 3, Contract No. 283286 under the Seventh Framework Programme of EU; the Austrian Federal Ministry of Science and Research BMBWK 650962/0001 VI/2/2009; the Romanian National Authority for Scientific Research, Contract No. 2-CeX 06-11-11/2006; the Grant-inAid for Specially Promoted Research (20002003), MEXT, Japan; the Austrian Science Fund (FWF): [P20651-N20] and [P24756-N20]; and the DFG Excellence Cluster Universe of the Technische Universität München.

REFERENCES

[1] SIDDHARTA Collaboration, *Phys. Lett.* **B704**, 113 (2011).
[2] SIDDHARTA Collaboration, *Nucl. Phys.* **A881**, 88 (2012).
[3] M. Bazzi *et al.*, *Nucl. Phys.* **A907**, 69 (2013).
[4] SIDDHARTA Collaboration, *Phys. Lett.* **B697**, 199 (2011).
[5] SIDDHARTA Collaboration, *Phys. Lett.* **B681**, 310 (2009).
[6] SIDDHARTA Collaboration, *Phys. Lett.* **B714**, 40 (2012).
[7] SIDDHARTA Collaboration, *Nucl. Phys.* **A914**, 305 (2013).
[8] SIDDHARTA Collaboration, *Nucl. Phys.* **A916**, 30 (2013).
[9] S. Bianco *et al.*, *Riv. Nuovo Cim.* **22**, 1 (1999).
[10] SIDDHARTA Collaboration, *Nucl. Instrum. Methods* **A581**, 326 (2007).
[11] M. Iwasaki *et al.*, *Phys. Rev. Lett.* **78**, 3067 (1997); T.M. Ito *et al.*, *Phys. Rev.* **C58**, 2366 (1998).
[12] G. Beer *et al.* [DEAR Collaboration], *Phys. Rev. Lett.* **94**, 212302 (2005).
[13] W. Weise, *Nucl. Phys.* **A835**, 51 (2010).
[14] SIDDHARTA-2 Collaboration, Proposal at Laboratori Nazionali di Frascati of INFN, "The upgrade of the SIDDHARTA apparatus for an enriched scientific case", 2010.

[15] C. Berucci *et al.*, Letter of Intent for J-PARC, "Measurement of the strong interaction induced shift and width of the 1s state of kaonic deuterium", 2013.

[16] C.J. Batty, *Nucl. Phys.* **A508**, 89 (1990).

[17] E. Friedman, *Hyperfine Interactions* **209**, 127 (2012) [arXiv:1111.7194v1 [nucl-th]].

[18] S. Baird *et al.*, *Nucl. Phys.* **A392**, 297 (1983).

[19] Y. Akaishi, in: Proceedings of the International Conference on Exotic Atoms (EXA05), http://dx.doi.org/10.1553/exa05s45

[20] M. Iwasaki *et al.*, *Nucl. Phys.* **A804**, 186 (2008).

[21] T. Suzuki *et al.*, *Phys. Rev.* **C76**, 068202 (2007).

[22] C.E. Wiegand, R. Pehl, *Phys. Rev. Lett.* **27**, 1410 (1971).

[23] C.J. Batty *et al.*, *Nucl. Phys.* **A326**, 455 (1979).

[24] S. Baird *et al.*, *Nucl. Phys.* **A392**, 297 (1983).

[25] S. Okada *et al.*, *Phys. Lett.* **B653**, 387 (2007).

[26] C.E. Wiegand, G.L. Godfrey, *Phys. Rev.* **A9**, 2282 (1974).

[27] C.E. Wiegand *et al.*, *Phys. Rev.* **A15**, 1780 (1977).